



OPEN

Prognostic Factors of Disease Recurrence in Breast Cancer Using Quantitative and Qualitative Magnetic Resonance Imaging (MRI) Parameters

Jeongmin Lee, Sung Hun Kim & Bong Joo Kang

The purpose of this study was to investigate prognostic factors predicting recurrence of breast cancer, focusing on imaging factors including morphologic features, quantitative MR parameters, and clinicopathologic factors. This retrospective study was approved by our institutional review board, and the requirement to obtain informed consent was waived. A total of 267 patients with breast cancer were enrolled in this study, who underwent dynamic contrast-enhanced magnetic resonance imaging (MRI) before surgery from February 2014 to June 2016. Imaging parameters of MRI, including morphologic features, perfusion parameters, and texture analysis, were retrospectively reviewed by two expert breast radiologists. Clinicopathologic information of enrolled patients was also reviewed using medical records. Univariable and multivariable Cox proportional hazards regression analyses were used to identify factors associated with cancer recurrence. C statistics was used to discriminate low and high risk patients for disease recurrence. Using Kaplan-Meier survival analysis, disease-free survival was compared between patients who experienced recurrence and those who did not. At a median follow up of 49 months, 32 patients (12%) showed disease: six cases of ipsilateral breast or axilla recurrence, one case of contralateral breast recurrence, 24 cases of distant metastasis, and one case of both ipsilateral breast recurrence and distant metastasis. Of multiple imaging features and parameters, increased ipsilateral vascularity and higher positive skewness of texture analysis showed significant association with disease recurrence in every multivariable model regardless of tumor subtype and pathologic stage. Pathologic stage, especially if higher than stage II, showed significant association with disease recurrence and its highest hazard ratio was 3.45 [95% confidence interval (CI): 1.37–8.67, $p = 0.008$]. Of the multivariable models, the model including clinico-pathologic factors and both qualitative and quantitative imaging parameters showed good discrimination with a high C index value of 0.825 (95% CI: 0.755–0.896). In addition, recurrence associated factors were associated with short interval time to disease recurrence by Kaplan-Meier survival analysis. Therefore, comprehensive analysis using both clinico-pathologic factors and qualitative and quantitative imaging parameters is more effective in predicting breast cancer recurrence. Among those factors, higher pathologic stage, increased ipsilateral vascularity and higher positive skewness of texture analysis could be good predictors of breast cancer recurrence. Moreover, when these three factors are applied comprehensively, they may also be the predictors for poor survival.

Breast cancer is a leading cause of death among women worldwide and the second most common cancer in Korean women. However, with increased screening and development of treatment methods, breast cancer mortality rates have improved over the last few decades^{1,2}. Postoperative adjuvant systemic therapies including chemotherapy, hormone therapy, and target agents have contributed to improving mortality rates in breast cancer patients^{3–5}.

Department of Radiology, Seoul St. Mary's Hospital, College of Medicine, The Catholic University of Korea, Seoul, Republic of Korea. ✉e-mail: rad-ksh@catholic.ac.kr

Despite such improvements, women who have previously undergone breast cancer treatment are at higher risk of breast cancer than those without history of breast cancer. In addition, patients with recurrent breast cancer have worse prognoses than those who have not recurred^{6–8}. For this reason, many efforts to predict prognosis in breast cancer patients including those with cancer recurrence have been made.

Oncotype DX (Genomic Health, Redwood City, CA, USA), a commercially available 21-gene breast cancer recurrence score assay, was recently introduced to predict prognosis in early breast cancer (estrogen receptor-positive/human epidermal growth factor receptor 2-negative/lymph node-negative) patients⁹. Recurrence score, calculated according to Oncotype DX, can help determine the direction of treatment in early breast cancer patients who need adjuvant systemic therapy after surgery¹⁰. However, Oncotype DX is limited in indications and expensive, making it difficult to apply to all breast cancer patients. In fact, Oncotype DX is performed only in one-third of eligible breast cancer patients in United States, and less than 20% of patients in European countries^{11,12}.

Breast MRI is performed in most patients with newly diagnosed breast cancer and can both diagnose breast cancer accurately and predict cancer prognosis using variable imaging features. Previous studies identified that several imaging features including rim enhancement pattern of tumor^{13,14}, presence of peritumoral edema on T2-weighted image^{15,16}, higher degree of background parenchymal enhancement (BPE), and increased vascularity around the tumor, indicate poor prognosis in breast cancer^{13–17}. In addition to morphologic features of tumor, quantitative MRI parameters derived from advanced MR techniques have been recently developed for prediction of breast cancer prognosis. For example, perfusion parameters derived from dynamic contrast-enhanced MRI (DCE-MRI) and tumor heterogeneity based on texture analysis can predict cancer prognosis^{18,19}. Such quantitative parameters may be more objective indicators than morphologic characteristics for predicting cancer prognosis.

Therefore, the purpose of this study is to investigate prognostic factors that predict breast cancer recurrence comprehensively, using MR morphologic features and quantitative MR parameters in addition to clinicopathologic factors.

Results

Patients. At a median follow up of 49 months (range 1 to 64 months), there were 32 cases (12%) of cancer recurrence (median 28.5 months, range 1 to 63 months): six cases of recurrence in the ipsilateral breast or axillary lymph node, one case in the contralateral side breast, 24 cases of distant metastases, and one case of recurrence both in the ipsilateral breast and distant metastasis. The median age of patients diagnosed with recurrent cancer was 48.5 (range, 25 to 74 years), and that of patients without disease recurrence was 51 years (range, 24 to 86 years), which were not significantly different ($p = 0.468$). Regarding immunohistochemical staining subtype, luminal B type was the most common subtype across all patients (124 of 267, 46.8%) as well as in the recurrence group (18 of 32, 56.3%). Regarding pathologic stage, stage II was the most common in the non-recurrent group (116 of 235, 49.6%), while stage III was most common in the recurrent group (12 of 32, 38.7%). Other characteristics of the 267 patients are summarized in Table 1.

Of 32 patients who had disease recurrence, three died within 17 months after recurrence was diagnosed, and three showed disease progressions. All of these patients had distant metastases. Twenty five patients remained disease-free after appropriate adjuvant treatment – hormonal therapy, chemotherapy, or radiation therapy – or repeat surgery. Only one patient was unable to follow-up after disease recurrence diagnosis.

Recurrence-associated factors. We assessed factors associated with disease recurrence according to the univariable and multivariable Cox proportional hazard regressions. Imaging parameters and clinical factors with p value less than 0.05 in univariable analysis were included as input parameters for multivariable analysis; pathologic stage, presence of rim enhancement, ipsilateral increased vascularity, skewness of texture analysis, and 25th percentile of Kep of perfusion parameters (Table 2). Tumor subtype was included in the final multivariable model despite not being statistically significant in univariable model because of its significant clinical relevance.

Model A was composed of clinicopathologic factors, including tumor subtype and pathologic stage. In model A, stage III and IV showed significant correlation with disease recurrence. The higher the pathologic stage was, the greater the correlation with disease recurrence was. Model B was composed of morphologic features including rim enhancement and ipsilateral vascularity, and clinico-pathologic factors including pathologic stage and tumor subtype. There was a significant correlation with the recurrence of disease in cases with increased ipsilateral vascularity (≥ 3), whereas rim enhancement showed no association with disease recurrence in model B. Model C was composed of quantitative parameters including skewness of texture analysis, 25th percentile of Kep of perfusion parameters and clinico-pathologic factors including pathologic stage and tumor subtype. In model C, higher skewness of texture analysis and higher Kep 25th percentile value showed significant correlation with disease recurrence. Finally, Model D included all clinicopathologic factors, morphologic features and quantitative MR parameters; pathologic stage, tumor subtype, ipsilateral vascularity, rim enhancement and skewness of texture analysis and 25th percentile of Kep of perfusion parameters. In model D, increased ipsilateral vascularity (≥ 3) and higher positive skewness of texture analysis were independently associated with disease recurrence (Table 3).

Comparison of C index of each model revealed that model D, including all clinicopathologic and imaging factors, showed the highest C index (0.825 [95% CI: 0.755–0.896]) with excellent discrimination for high risk group of recurrence. Model B also showed excellent discriminative power for high risk group of recurrence with C index of 0.800 (95% CI: 0.724–0.876). Model C also showed acceptable discrimination with C index of 0.752 (95% CI: 0.655–0.848). When the C index of model B, C, D were compared to that of model A, model D showed the highest C index and barely escaped being statistically significant at the 5% risk level ($p = 0.052$). Model B and C also showed higher C index than that of model A, although without significance (Table 4).

	Total (n = 267)	Non-recurrent (n = 235)	Recurrence (n = 32)	p value
Patient age				
mean \pm SD.	50.7 \pm 10.8	50.9 \pm 10.7	49.6 \pm 11.6	0.468
Median(IQR)	51.0 (43.0–58.0)	51.0 (43.0–58.0)	48.5 (41.5–56.5)	
Menopausal status				
premenopause	133 (50.0)	114 (48.7)	19 (59.4)	0.258
postmenopause	133 (50.0)	120 (51.3)	13 (40.6)	
Imaging				
Rim enhancement				
No	178 (66.7)	162 (68.9)	16 (50.0)	0.033
Yes	89 (33.3)	73 (31.1)	16 (50.0)	
Peritumoral edema				
No	163 (61.1)	145 (61.7)	18 (56.3)	0.553
Yes	104 (39.0)	90 (38.3)	14 (43.8)	
BPE grade				
minimal	143 (53.8)	125 (53.4)	18 (56.3)	0.144
mild	53 (19.9)	51 (21.8)	2 (6.3)	
moderate	43 (16.2)	35 (15.0)	8 (25.0)	
marked	27 (10.2)	23 (9.8)	4 (12.5)	
Ipsilateral vascularity				
Mean \pm SD	2.0 \pm 1.8	1.9 \pm 1.7	3.0 \pm 2.4	0.010
Median (IQR)	2.0 (1.0–3.0)	2.0 (0.0–3.0)	3.0 (1.0–5.0)	
Immunohistochemical staining				
Subtype				
luminal A	63 (23.8)	58 (24.9)	5 (15.6)	0.314
luminal B	124 (46.8)	106 (45.5)	18 (56.3)	
HER2 +	34 (12.8)	32 (13.7)	2 (6.3)	
Triple negative cancer (TNC)	44 (16.6)	37 (15.9)	7 (21.9)	
Staging				
0	13 (4.9)	13 (5.6)	0 (0.0)	0.001
I	77 (29.1)	70 (29.9)	7 (22.6)	
II	126 (47.6)	116 (49.6)	10 (32.3)	
III	45 (17.0)	33 (14.1)	12 (38.7)	
IV	4 (1.5)	2 (0.9)	2 (6.5)	
Texture analysis				
Kurtosis				
Mean \pm SD	2.9 \pm 0.7	2.9 \pm 0.7	2.9 \pm 0.8	0.802
Median(IQR)	2.8 (2.5–3.2)	2.8 (2.5–3.2)	2.7 (2.5–3.2)	
Skewness				
Mean \pm SD	–0.1 \pm 0.4	–0.1 \pm 0.4	0.0 \pm 0.4	0.031
Median (IQR)	–0.1 (–0.3–0.1)	–0.2 (–0.4–0.1)	–0.1 (–0.2–0.3)	
Entropy				
Mean \pm SD	2.0 \pm 0.6	2.0 \pm 0.6	2.1 \pm 0.5	0.359
Median (IQR)	1.9 (1.6–2.4)	1.9 (1.6–2.4)	2.0 (1.8–2.5)	
Perfusion parameters				
<i>K</i>_{trans}				
25percentile				
Mean \pm SD	0.2 \pm 0.1	0.2 \pm 0.1	0.2 \pm 0.1	0.325
Median (IQR)	0.1 (0.1–0.2)	0.1 (0.1–0.2)	0.2 (0.1–0.2)	
50percentile				
Mean \pm SD	0.3 \pm 0.2	0.3 \pm 0.2	0.3 \pm 0.1	0.929
Median (IQR)	0.2 (0.2–0.3)	0.2 (0.2–0.3)	0.2 (0.2–0.4)	
75percentile				
Mean \pm SD	0.4 \pm 0.3	0.4 \pm 0.3	0.4 \pm 0.1	0.858
Median (IQR)	0.3 (0.2–0.5)	0.3 (0.2–0.5)	0.3 (0.2–0.5)	
Continued				

	Total (n = 267)	Non-recurrent (n = 235)	Recurrence (n = 32)	p value
Mean				
Mean ± SD	0.9 ± 9.7	1.0 ± 10.3	0.3 ± 0.1	0.962
Median (IQR)	0.2 (0.2–0.3)	0.2 (0.2–0.3)	0.2 (0.2–0.4)	
<i>Ke_p</i>				
25percentile				
Mean ± SD	0.3 ± 0.4	0.3 ± 0.4	0.3 ± 0.2	0.211
Median (IQR)	0.3 (0.2–0.4)	0.3 (0.2–0.4)	0.3 (0.2–0.4)	
50percentile				
Mean ± SD	0.6 ± 0.8	0.6 ± 0.9	0.5 ± 0.2	0.783
Median (IQR)	0.5 (0.4–0.6)	0.5 (0.4–0.6)	0.5 (0.4–0.6)	
75percentile				
Mean ± SD	0.9 ± 1.7	0.9 ± 1.8	0.8 ± 0.3	0.921
Median (IQR)	0.7 (0.5–0.9)	0.7 (0.5–0.9)	0.7 (0.6–0.9)	
mean				
Mean ± SD	0.7 ± 1.7	0.7 ± 1.8	0.6 ± 0.2	0.742
Median (IQR)	0.5 (0.4–0.7)	0.5 (0.4–0.7)	0.5 (0.5–0.6)	
<i>Ve</i>				
25percentile				
Mean ± SD	102.1 ± 1636.1	115.4 ± 1740.0	0.4 ± 0.1	0.197
Median (IQR)	0.4 (0.3–0.5)	0.4 (0.3–0.5)	0.4 (0.3–0.5)	
50percentile				
Mean ± SD	133.6 ± 2141.5	151.0 ± 2277.5	0.5 ± 0.2	0.681
Median (IQR)	0.5 (0.4–0.6)	0.5 (0.4–0.6)	0.5 (0.4–0.6)	
75percentile				
Mean ± SD	133.7 ± 2141.5	151.1 ± 2277.5	0.6 ± 0.2	0.960
Median (IQR)	0.6 (0.5–0.8)	0.6 (0.5–0.8)	0.6 (0.5–0.7)	
mean				
Mean ± SD	110.1 ± 1763.4	124.4 ± 1875.3	0.5 ± 0.2	0.611
Median (IQR)	0.5 (0.4–0.6)	0.5 (0.4–0.6)	0.5 (0.4–0.6)	

Table 1. Patient characteristics.

Survival analysis. Of the imaging parameters associated with disease recurrence, increased ipsilateral vascularity and skewness of texture analysis were associated with worse DFS in Kaplan-Meier analysis. Patients with increased vascularity (≥ 3) on MRI had shorter recurrence intervals ($p = 0.002$) than those without increased vascularity (< 3) on MRI. Patients with higher positive skewness ($p = 0.005$) in texture analysis showed lower DFS. We observed lower DFS in patients with triple negative subtype cancer compared to those with other subtypes, but the difference was not significant ($p = 0.243$) (Fig. 1).

In addition to MRI parameters, the pathologic stage was associated with worse DFS ($p = 0.002$). In other words, higher pathologic stage of initial breast cancer was associated with worse DFS.

Discussion

With the advancement of MR technology, it has become easier to obtain various qualitative parameters. Perfusion parameters and texture analysis are representative quantitative parameters that are being used to predict disease prognosis. In this study, we tried to predict disease recurrence using both qualitative morphologic features of MRI and quantitative MR parameters. Of several multivariable models, the comprehensive model showed that, increased ipsilateral vascularity and skewness of texture analysis are associated with disease recurrence independently with the best discriminative performance.

Increased vascularity of the tumor-involved breast is related to neoangiogenesis in tumors. Increase in the number of vessels around the tumor contribute to hematogenous spread of tumor cells and distant metastasis of tumors²⁰. For this reason, increased vascularity around a tumor may be associated with disease recurrence and worse DFS, as shown in the present study. Also, increased vascularity always showed significant association with disease recurrence in every multivariable model. Increased vascularity due to the tumor can affect other MRI parameters related to tumor vascularity, including perfusion or texture parameters^{13,19}. However, texture and perfusion parameters were associated with disease recurrence independent of increased ipsilateral vascularity in present study.

Generally higher entropy, kurtosis, and positive skewness of the tumor in DCE-MRI suggest poor prognosis in texture analysis^{21,22}. Especially for skewness, it represents a measure of asymmetry of probability distribution. Higher positive skewness could mean long right-sided tail with lower mean value in histogram. In our study, it could mean that lower mean signal intensity (SI) in the fat-saturated contrast enhanced T1 weighted images (WI). Low SI of tumor in fat-saturated contrast enhanced T1WI may suggested the situation such tumor necrosis.

	HR (95% CI)	p value
Clinicopathologic Factors		
Patient age (≤ 40)	0.66 (0.27–1.59)	0.352
Menopausal status	0.71 (0.35–1.44)	0.341
Subtype		0.328
Luminal A	Reference	
Luminal B	1.67 (0.62–4.49)	0.309
Her2 +	0.83 (0.18–3.86)	0.808
TNC	2.44 (0.78–7.62)	0.124
Staging		0.002
0	0.37 (0.02–7.02)	0.504
I	1.20 (0.45–3.19)	0.713
II	Reference	
III	3.64 (1.54–8.58)	0.003
IV	9.31 (2.20–39.43)	0.003
Morphologic features		
Rim enhancement		
No	Reference	
Yes	2.02 (1.01–4.05)	0.047
Peritumoral edema		
No	Reference	
Yes	1.32 (0.66–2.65)	0.438
BPE grade		0.155
Minimal	Reference	
Mild	0.37 (0.09–1.45)	0.154
Moderate	1.75 (0.75–4.09)	0.194
Marked	1.63 (0.56–4.76)	0.376
Ipsilateral vascularity		
<3	Reference	
≥ 3	2.85 (1.41–5.74)	0.003
Quantitative parameters[†]		
Texture analysis		
Kurtosis		
<3.61	Reference	
≥ 3.61	1.79 (0.70–4.55)	0.223
Skewness		
<0.29	Reference	
≥ 0.29	2.97 (1.37–6.43)	0.006
Entropy		
<1.82	Reference	
≥ 1.82	2.00 (0.90–4.44)	0.089
Perfusion parameters		
Ktrans		
25percentile		
<0.16	Reference	
≥ 0.16	1.53 (0.75–3.13)	0.244
50percentile		
<0.42	Reference	
≥ 0.42	0.28 (0.05–1.47)	0.132
75percentile		
<0.58	Reference	
≥ 0.58	0.11 (0.01–1.87)	0.126
mean		
<0.43	Reference	
≥ 0.43	0.12 (0.01–2.02)	0.14
Continued		

	HR (95% CI)	p value
Ke_p		
25percentile		
<0.20	Reference	
≥0.20	3.12 (1.01–9.68)	0.049
50percentile		
<0.61	Reference	
≥0.61	0.65 (0.27–1.57)	0.336
75percentile		
<0.55	Reference	
≥0.55	2.26 (0.82–6.25)	0.116
mean		
<0.45	Reference	
≥0.45	1.93 (0.84–4.46)	0.123
Ve		
25 percentile		
<0.20	Reference	
≥0.20	6.99 (0.41–119.97)	0.18
50 percentile		
<0.55	Reference	
≥0.55	1.65 (0.81–3.39)	0.169
75 percentile		
<0.73	Reference	
≥0.73	0.56 (0.23–1.35)	0.195
mean		
<0.53	Reference	
≥0.53	1.65 (0.80–3.38)	0.172

Table 2. Univariable Cox proportional hazards regression. †Optimal cut-off value of each quantitative parameter was determined using maximally selected rank statistics.

Considering tumor necrosis is often accompanied in high grade tumor with poor prognosis, higher positive skewness may suggest poor prognosis.

As shown in result, multivariable Cox proportional hazard model using clinicopathologic factors and both morphologic feature and quantitative parameters showed the highest and excellent discriminative ability (C index 0.825, [95% CI: 0.755–0.896]) among multivariable models. The C index of the comprehensive model was higher than that of the model with clinico-pathologic factors alone with statistical relevance. Also, although not statistically significant, the comprehensive model showed higher C index than the model with morphologic feature and clinico-pathologic factors. In other words, applying advanced MR parameters to the previously known clinico-pathological predictors and morphologic imaging characteristics could be more helpful to predict disease recurrence.

The imaging parameters which were associated with disease recurrence, also showed association with lower DFS in Kaplan-Meier analysis. Some previous studies suggested that patients with shorter interval between surgery and first relapse had shorter overall survival in breast cancer^{23–25}. In other words, DFS itself is an important prognostic factor that can predict overall survival in recurred patients. In our study, recurrent diseases were confirmed mostly within 3 years (mean 31 months, median 28.5 months) after first preoperative MRI. Of 32 patients with disease recurrence, three died within 17 months. Although it is difficult to analyze overall survival due to the small number of expired cases in our study, it would be possible to obtain imaging parameters related to overall survival with more patients and a longer follow-up period.

There are a number of limitations of the present study. It was a retrospective, single-center study with a small number of patients with disease recurrence. The disease recurrence event number was much smaller than the number of total patients. This can weaken the representativeness of results. In addition, due to differences in follow-up period after surgery, disease recurrence may not have been fully investigated at the time of review. Also, basic information about the tumor, such as other morphologic features following the BI-RADS lexicon and kinetic curve pattern, was not included in the present study, despite being possible prognostic factors of disease recurrence.

We investigated morphologic features, quantitative MR parameters and clinicopathologic factors to predict disease recurrence in breast cancer patients. The present study analyzed multiple imaging prognostic factors more comprehensively that has been previously performed. We found that higher pathologic stage, increased ipsilateral vascularity and higher positive skewness of texture analysis were associated with disease recurrence independent of tumor subtype, and using quantitative MR parameters in addition to clinicopathologic factors and morphologic features could be helpful to predict disease recurrence more accurately. We expect that these results will help physicians predict the prognosis of breast cancer patients and choose appropriate treatment methods more easily, and ultimately will contribute to improving survival of breast cancer patients.

	adjusted HR (95% CI)	p value
Model A		
Subtype		
Luminal A	Reference	
Luminal B	1.46 (0.54–3.95)	0.462
Her2 +	0.87 (0.19–4.01)	0.856
TNC	1.57 (0.47–5.22)	0.46
pTNM		
0	0.51 (0.03–9.79)	0.652
I	1.23 (0.46–3.28)	0.673
II	Reference	
III	3.63 (1.53–8.58)	0.003
IV	7.89 (1.79–34.68)	0.006
Model B		
Subtype		
Luminal A	Reference	
Luminal B	1.40 (0.51–3.83)	0.518
Her2 +	0.57 (0.12–2.71)	0.476
TNC	1.43 (0.42–4.85)	0.566
pTNM		
0	1.96 (0.10–38.63)	0.658
I	1.56 (0.08–30.19)	0.768
II	Reference	
III	5.46 (0.29–104.18)	0.259
IV	9.28 (0.37–231.50)	0.175
Rim enhancement		
No	Reference	
Yes	1.58 (0.74–3.38)	0.234
Ipsilateral vascularity		
<3	Reference	
≥3	2.67 (1.28–5.60)	0.009
Model C		
Subtype		
Luminal A	Reference	
Luminal B	1.84(0.66–5.15)	0.246
Her2 +	0.81(0.17–3.80)	0.787
TNC	2.56(0.73–8.98)	0.141
pTNM		
0	0.58(0.03–11.53)	0.723
I	1.45(0.53–3.96)	0.470
II	Reference	
III	3.59(1.44–9.00)	0.006
IV	3.86(0.79–18.85)	0.095
Texture analysis: Skewness		
<0.29	Reference	
≥0.29	2.85(1.17–6.94)	0.021
Kep: 25perc		
<0.20	Reference	
≥0.20	3.84(1.16–12.72)	0.028
Model D		
Subtype		
Luminal A	Reference	
Luminal B	1.71 (0.60–4.88)	0.317
Her2 +	0.53 (0.11–2.61)	0.437
TNC	1.96 (0.54–7.06)	0.306
Continued		

	adjusted HR (95% CI)	p value
pTNM		
0	0.85 (0.04–16.96)	0.913
I	1.46 (0.53–4.05)	0.465
II	Reference	
III	3.45 (1.37–8.67)	0.008
IV	3.27 (0.67–16.00)	0.144
Rim enhancement		
No	Reference	
Yes	2.09 (0.92–4.76)	0.08
Ipsilateral vascularity		
<3	Reference	
≥3	2.71 (1.25–5.86)	0.011
Texture analysis: Skewness		
<0.29	Reference	
≥0.29	3.21 (1.26–8.23)	0.015
Ke_p: 25perc		
<0.20	Reference	
≥0.20	2.66 (0.82–8.67)	0.105

Table 3. Multivariable Cox proportional hazards regression.

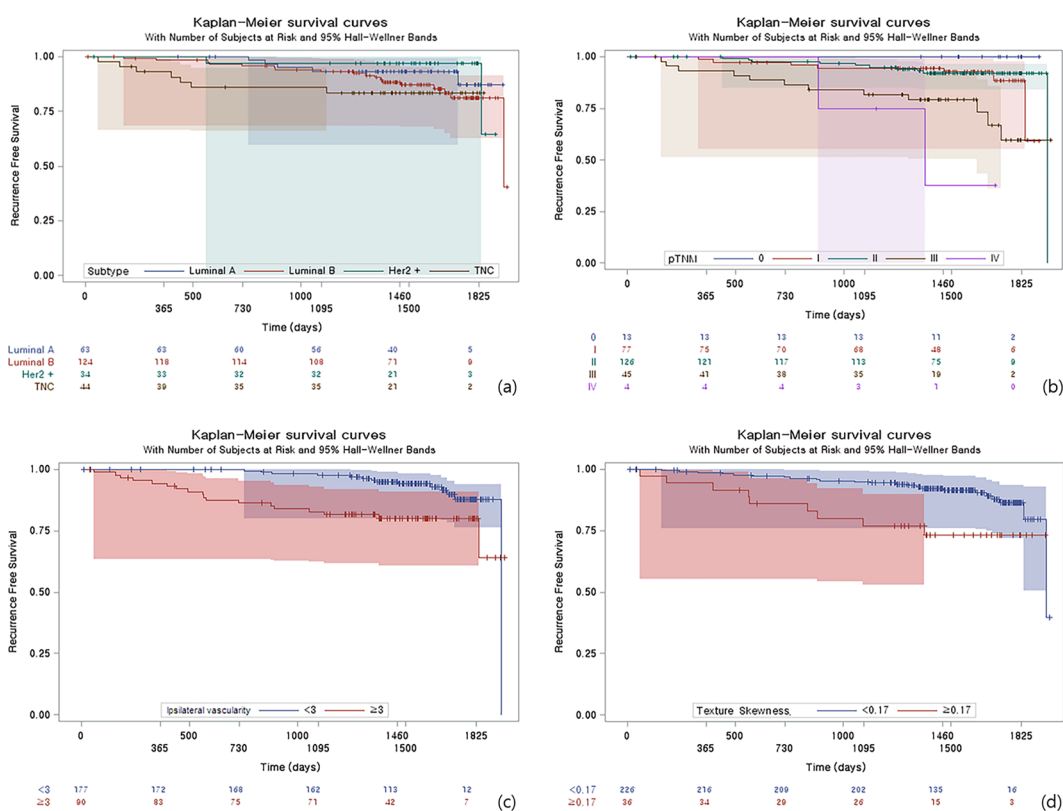


Figure 1. Kaplan-Meier survival curves according to (a) tumor subtype, (b) pathologic stage, (c) ipsilateral vascularity, (d) skewness. Higher pathologic stage (over stage II, $p < 0.001$), increased ipsilateral vascularity (≥ 3 , $p < 0.002$), higher positive skewness (≥ 0.29 $p = 0.005$) were associated with worse DFS.

Materials and Methods

Patients. This study was approved by the Institutional Review Board of Seoul St. Mary’s Hospital. The requirement for informed consent was waived due to its retrospective nature and it was confirmed by IRB of our institution. Investigations were carried out as per the rules of the Declaration of Helsinki of 1975, revised in 2013.

Model	Harrell's C index (95% CI)	p value
Model A	0.698 (0.590–0.805)	Reference
Model B	0.800(0.724–0.876)	0.128
Model C	0.752(0.655–0.848)	0.464
Model D	0.825 (0.755–0.896)	0.052

Table 4. C statistics of multivariable Cox proportional hazards regression models.

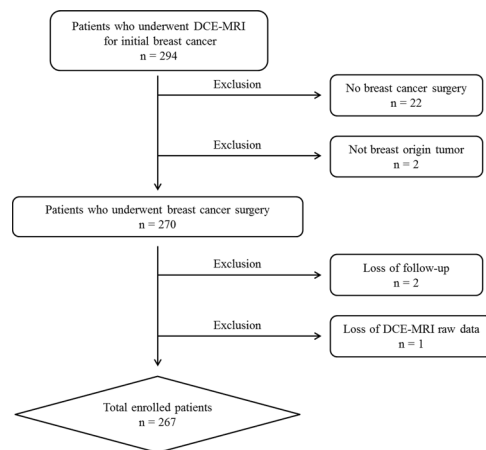


Figure 2. Study population with exclusion criteria.

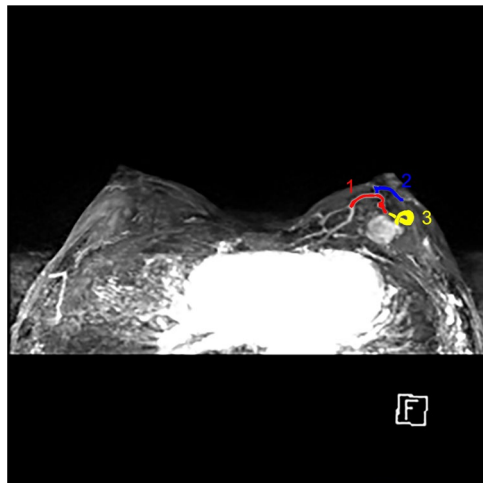


Figure 3. MIP images show prominent vessels of left breast with enhancing tumor at mid upper portion of left breast. According to our criteria, the number of vessels counted is three.

A total of 294 breast cancer patients who underwent breast DCE-MRI between February 2014 and May 2016 was included in the study sample. Of 294 patients, 22 who had not undergone surgery for breast cancer were excluded. Two patients with cancers that were not breast cancer were also excluded. Of the remaining 270 patients, two who were lost to follow-up for more than one year and one without raw MR data were excluded. Finally, 267 patients were enrolled in our study (Fig. 2). All enrolled patients were treated according to standard treatment guidelines for breast cancer. Only one lesion was analyzed per patient. In cases of bilateral or multiple breast cancers, the largest lesion was analyzed as a target lesion.

Clinicopathologic information. We reviewed the medical records of all 267 patients. Clinical information comprised patient age, menopausal status, date of pretreatment MRI scanning, and date of last visit to the outpatient clinic. For calculation of disease-free survival, we considered the date of pretreatment MRI scanning to be the first day of diagnosis. Generally, MRI scanning was performed 10 to 14 days after biopsy. Pathologic information for initial breast cancer was obtained from surgical specimens, including hormonal receptor status, Ki-67 index, and presence of lymphovascular invasion. Pathologic stage was determined based on the AJCC 7th edition.



Figure 4. On axial T2-weighted image, high signal intensity which is defined as peritumoral edema, is noted at posterior aspect of breast tumor in left upper outer breast.

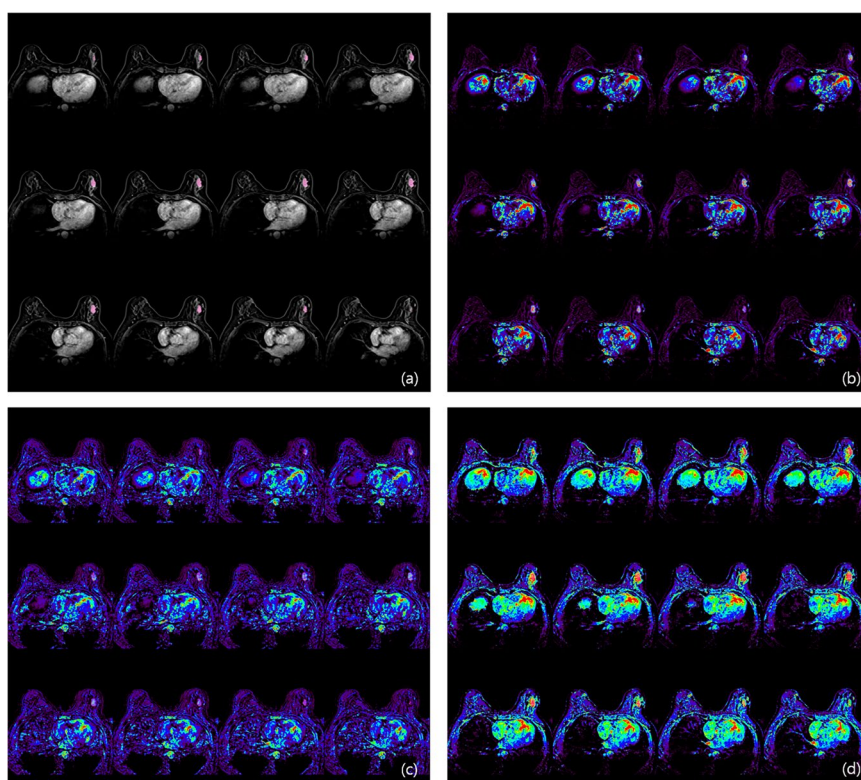


Figure 5. Evaluation of perfusion parameter. (a) On Fat-saturated T1-weighted images, tumor segmentation was performed with semi-automatic tool (magic wand tool). After applying tumor segmentation on Ktrans map (b), Kep map (c) and Ve map (d), perfusion parameters from each map were calculated.

Cancer recurrence was defined as newly diagnosed ipsilateral or contralateral breast cancer or distant metastasis after surgery. The day of confirmed recurrent cancer on biopsy was considered the date of recurrence. When biopsy data were not available, the date of recurring lesion detection by imaging scanning such as positron emission tomography (PET), bone scan, or computed tomography (CT) was considered the relapse date.

MRI protocol. MRI examinations were performed with patients in the prone position using a Magnetom Verio 3 T system (Siemens Healthcare, Erlangen, Germany) and a dedicated eight-channel phase-array coil. Images were obtained using the following sequences: (1) axial turbo spin-echo T2-weighted imaging (T2WI) with TR/TE of 4530/93 msec, flip angle of 80°, field of view (FOV) 320 × 320 mm², matrix size of 576 × 403, slice thickness of 4 mm, and acquisition time of 2 min 28 sec; (2) pre-contrast T1-weighted three-dimensional (3D) volumetric interpolated breath-hold examinations (3D VIBE) with TR/TE of 2.7/0.8 msec, FOV of 320 × 320 mm², matrix size of 256 × 192, slice thickness of 2 mm with various flip angles (2°, 6°, 9°, 12°, 15°), and acquisition time of 2 min 15 sec to determine tissue T1 relaxation time prior to the arrival of contrast agent; (3) dynamic



Figure 6. Texture analysis using 3D slicer. After tumor segmentation in the axial (a), coronal (b) and sagittal planes (c), texture parameters of tumor were calculated.

contrast-enhanced axial T1-weighted imaging (T1WI) with fat suppression with TR/TE of 2.5/0.8 msec, flip angle of 10°, slice thickness of 2.0 mm, and acquisition time of 5 min 30 sec (temporal resolution 6 sec) following an intravenous bolus injection of 0.1 mmol/kg gadobutol (Gadovist, Schering, Berlin, Germany) followed by a 20 ml saline flush; and (4) delayed axial T1-weighted 3D VIBE with TR/TE of 4.4/1.7 msec, flip angle of 10°, slice thickness of 1.2 mm, FOV of 340 mm, and matrix size of 448 × 358 to evaluate the overall extent of tumor.

Morphologic analysis. Two breast radiologists with 5 years and 20 years of experience in breast imaging retrospectively reviewed pretreatment breast MRI using a picture archiving and communication system (PACS) (Maroview 5.4; Innitt, Seoul, Korea) and workstation monitor.

Enhancement pattern and background parenchymal enhancement (BPE). The internal enhancement pattern (rim or non-rim) of the tumor and BPE degree (minimal/mild or moderate/marked) were analyzed following the guidelines of the fifth edition of the Breast Imaging Reporting and Data System (BI-RADS) MRI lexicon²⁶. Cases of cancer expressed as non-mass enhancement only were considered negative for rim enhancement.

Ipsilateral vascularity. The number of vessels around the tumor was measured in maximum-intensity-projection (MIP) reconstruction views to reduce confusion caused by BPE. Only vessels 3 cm or longer in length and 2 mm or larger in maximal transverse diameter were recognized as target vessels. We counted the number of vessels visualized in the breast containing the index cancer (Fig. 3). In cases of bilateral or multiple breast cancers, the number of vessels in the breast that contained the largest tumor were counted¹³.

Peritumoral edema. Peritumoral edema was defined as increased signal intensity around the tumor or high signal intensity that is similar to water or vessel signal intensity, posterior to the tumor in the prepectoral area in

T2-weighted images. Peritumoral edema was evaluated by visual evaluation on the PACS system by both readers (Fig. 4)^{15,16}.

MR parameters. *Perfusion parameters.* A standard Tofts model was used to evaluate perfusion parameters on DCE-MRI. Methods used to analyze perfusion parameters were described in a previous study (Fig. 5)²⁷.

Texture analysis parameters. For texture analysis, we used free and open source software package for visualization and medical image computing (3D slicer, ver. 4.8.0; available at: <https://slicer.org/>), with dynamic contrast-enhanced T1-weighted images with fat saturation derived from the PACS system. Contrast-enhanced T1-weighted images acquired 80 seconds after contrast material injection were assessed. After selection of the enhancing tumor, semiautomatic tumor segmentation was performed, and 19 texture features were extracted automatically. Among these 19 features, we selected entropy, skewness, and kurtosis to evaluate tumor heterogeneity. In cases of multifocal, multicentric, or bilateral cancer, texture analysis was performed for the largest tumor (Fig. 6).

Statistical analysis. Using univariable and multivariable Cox proportional hazard regression analyses, we estimated hazard ratios with 95% confidence intervals (CI)s for disease recurrence according to imaging parameters and clinicopathological factors. First, univariable Cox proportional hazard regression analysis was performed for each parameter. Then, multivariable Cox proportional hazard regression analysis was performed using parameters with $p < 0.05$ in univariable analysis and other parameters of known clinical relevance. Stepwise selection was applied to control multicollinearity and determine the final model^{28,29}.

Because tumor subtype may affect imaging features of tumors on MRI, multivariable models were built to exclude the effects of clinical factors on imaging parameters. Multivariable models were composed in four ways: clinico-pathologic factors alone, qualitative parameters with clinico-pathologic factors, quantitative parameters with clinico-pathologic factors, and qualitative and quantitative imaging parameters, and clinico-pathologic factors. In multivariable analysis, parameters with $p < 0.05$ were considered statistically significant.

The C statistics was used for discrimination of high and low risk patients for disease recurrence. The C statistics value ranges from 0.5 (no discrimination) to 1.0 (perfect discrimination). According to Hosmer and Lemeshow, all values were interpreted as acceptable discrimination (0.7–0.8), excellent discrimination (0.8–0.9), and outstanding discrimination (≥ 0.9). The C statistic values of each model of multivariable regression analysis were compared³⁰.

Missing data were deleted pairwise, minimizing loss of data by using all available cases for each analysis (missing rate: less than 6.5% of kinetic parameters and less than 3% of otherwise). To determine optimal cutoff values of imaging parameters to predict recurrence, we used maximally selected rank statistics.

Kaplan-Meier estimates were used for comparison of disease-free survival (DFS) between the recurrent group and non-recurrent group using imaging parameters and clinicopathological factors that were significant in univariable Cox proportional hazards regression. Survival differences were compared using log rank test.

Statistical analyses were performed using SAS version 9.4 (SAS Institute, Cary, North Carolina, USA) and the R “maxstat” package in R version 2.15.3 (R Foundation, Vienna, Austria; <http://www.R-project.org>).

Received: 28 April 2019; Accepted: 8 April 2020;

Published online: 05 May 2020

References

- Jung, K. W., Won, Y. J., Kong, H. J. & Lee, E. S., Community of Population-Based Regional Cancer, R. Cancer Statistics in Korea: Incidence, Mortality, Survival, and Prevalence in 2015. *Cancer Res. Treat.* **50**, 303–316, <https://doi.org/10.4143/crt.2018.143> (2018).
- DeSantis, C., Ma, J., Bryan, L. & Jemal, A. Breast cancer statistics, 2013. *CA Cancer J. Clin.* **64**, 52–62, <https://doi.org/10.3322/caac.21203> (2014).
- Kalager, M., Zelen, M., Langmark, F. & Adami, H. O. Effect of screening mammography on breast-cancer mortality in Norway. *N. Engl. J. Med.* **363**, 1203–1210, <https://doi.org/10.1056/NEJMoa1000727> (2010).
- Bleyer, A. & Welch, H. G. Effect of three decades of screening mammography on breast-cancer incidence. *N. Engl. J. Med.* **367**, 1998–2005, <https://doi.org/10.1056/NEJMoa1206809> (2012).
- Autier, P., Boniol, M., Gavin, A. & Vatten, L. J. Breast cancer mortality in neighbouring European countries with different levels of screening but similar access to treatment: trend analysis of WHO mortality database. *BMJ* **343**, d4411, <https://doi.org/10.1136/bmj.d4411> (2011).
- Wapnir, I. L. *et al.* Prognosis after ipsilateral breast tumor recurrence and locoregional recurrences in five National Surgical Adjuvant Breast and Bowel Project node-positive adjuvant breast cancer trials. *J. Clin. Oncol.* **24**, 2028–2037, <https://doi.org/10.1200/JCO.2005.04.3273> (2006).
- Anderson, S. J. *et al.* Prognosis after ipsilateral breast tumor recurrence and locoregional recurrences in patients treated by breast-conserving therapy in five National Surgical Adjuvant Breast and Bowel Project protocols of node-negative breast cancer. *J. Clin. Oncol.* **27**, 2466–2473, <https://doi.org/10.1200/JCO.2008.19.8424> (2009).
- Fourquet, A. *et al.* Prognostic factors of breast recurrence in the conservative management of early breast cancer: a 25-year follow-up. *Int. J. Radiat. Oncol. Biol. Phys.* **17**, 719–725 (1989).
- Paik, S. *et al.* A multigene assay to predict recurrence of tamoxifen-treated, node-negative breast cancer. *N. Engl. J. Med.* **351**, 2817–2826, <https://doi.org/10.1056/NEJMoa041588> (2004).
- Lee, M. H. *et al.* The clinical impact of 21-gene recurrence score on treatment decisions for patients with hormone receptor-positive early breast cancer in Korea. *Cancer Res. Treat.* **47**, 208–214, <https://doi.org/10.4143/crt.2013.223> (2015).
- Orucevic, A., Heidel, R. E. & Bell, J. L. Utilization and impact of 21-gene recurrence score assay for breast cancer in clinical practice across the United States: lessons learned from the 2010 to 2012 National Cancer Data Base analysis. *Breast Cancer Res. Treat.* **157**, 427–435, <https://doi.org/10.1007/s10549-016-3833-9> (2016).

12. Albanell, J. *et al.* Pooled analysis of prospective European studies assessing the impact of using the 21-gene Recurrence Score assay on clinical decision making in women with oestrogen receptor-positive, human epidermal growth factor receptor 2-negative early-stage breast cancer. *Eur. J. Cancer* **66**, 104–113, <https://doi.org/10.1016/j.ejca.2016.06.027> (2016).
13. Choi, E. J., Choi, H., Choi, S. A. & Youk, J. H. Dynamic contrast-enhanced breast magnetic resonance imaging for the prediction of early and late recurrences in breast cancer. *Medicine* **95**, e5330, <https://doi.org/10.1097/MD.0000000000005330> (2016).
14. Schmitz, A. M., Loo, C. E., Wesseling, J., Pijnappel, R. M. & Gilhuijs, K. G. Association between rim enhancement of breast cancer on dynamic contrast-enhanced MRI and patient outcome: impact of subtype. *Breast Cancer Res. Treat.* **148**, 541–551, <https://doi.org/10.1007/s10549-014-3170-9> (2014).
15. Bae, M. S. *et al.* Pretreatment MR Imaging Features of Triple-Negative Breast Cancer: Association with Response to Neoadjuvant Chemotherapy and Recurrence-Free Survival. *Radiology* **281**, 392–400, <https://doi.org/10.1148/radiol.2016152331> (2016).
16. Hyejin, C. *et al.* Invasive Breast Cancer: Prognostic Value of Peritumoral Edema Identified at Preoperative MR Imaging. *Radiology* **287**(1), 68–75 (2018).
17. Lim, Y. *et al.* Background parenchymal enhancement on breast MRI: association with recurrence-free survival in patients with newly diagnosed invasive breast cancer. *Breast Cancer Res. Treat.* **163**, 573–586, <https://doi.org/10.1007/s10549-017-4217-5> (2017).
18. Koo, H. R. *et al.* Correlation of perfusion parameters on dynamic contrast-enhanced MRI with prognostic factors and subtypes of breast cancers. *J. Magn. Reson. Imaging* **36**, 145–151, <https://doi.org/10.1002/jmri.23635> (2012).
19. Kim, J. H. *et al.* Breast Cancer Heterogeneity: MR Imaging Texture Analysis and Survival Outcomes. *Radiology* **282**, 665–675, <https://doi.org/10.1148/radiol.2016160261> (2017).
20. Heimann, R., Ferguson, D., Gray, S. & Hellman, S. Assessment of intratumoral vascularization (angiogenesis) in breast cancer prognosis. *Breast Cancer Res. Treat.* **52**, 147–158 (1998).
21. Just, N. Improving tumour heterogeneity MRI assessment with histograms. *Br. J. Cancer* **111**, 2205–2213, <https://doi.org/10.1038/bjc.2014.512> (2014).
22. Alic, L., Niessen, W. J. & Veenland, J. F. Quantification of heterogeneity as a biomarker in tumor imaging: a systematic review. *PLoS One* **9**, e110300, <https://doi.org/10.1371/journal.pone.0110300> (2014).
23. Kim, H. *et al.* Prognostic factors for survivals from first relapse in breast cancer patients: analysis of deceased patients. *Radiat. Oncol. J.* **31**, 222–227, <https://doi.org/10.3857/roj.2013.31.4.222> (2013).
24. Clark, G. M., Sledge, G. W. Jr., Osborne, C. K. & McGuire, W. L. Survival from first recurrence: relative importance of prognostic factors in 1,015 breast cancer patients. *J. Clin. Oncol.* **5**, 55–61, <https://doi.org/10.1200/JCO.1987.5.1.55> (1987).
25. Vogel, C. L., Azevedo, S., Hilsenbeck, S., East, D. R. & Ayub, J. Survival after first recurrence of breast cancer. The Miami experience. *Cancer* **70**, 129–135 (1992).
26. Morris EA, C. C. *et al.* ACR BI-RADS[®] Magnetic Resonance Imaging. In: ACR BI-RADS[®] Atlas, Breast Imaging Reporting and Data System. (American College of Radiology, 2013).
27. Lee, J., Kim, S. H. & Kang, B. J. Pretreatment prediction of pathologic complete response to neoadjuvant chemotherapy in breast cancer: Perfusion metrics of dynamic contrast enhanced MRI. *Sci. Rep.* **8**, 9490, <https://doi.org/10.1038/s41598-018-27764-9> (2018).
28. Heinze, G. & Schemper, M. A solution to the problem of monotone likelihood in Cox regression. *Biometrics* **57**, 114–119 (2001).
29. Heinze, G. & Ploner, M. SAS and SPLUS programs to perform Cox regression without convergence problems. *Comput. Methods Prog. Biomed.* **67**, 217–223 (2002).
30. Hosmer DW, L. S. *Applied logistic regression*. 142–162 (New York, NY: Wiley, 2000).

Acknowledgements

This study was funded by Reyon Pharmaceutical, Co., Ltd. (Seoul, Korea). The statistical consultation was supported by Department of Biostatistics of the Catholic Research Coordinating Center, Catholic Medical Center, South Korea.

Author contributions

Guarantor of integrity of the entire study: Sung Hun Kim, Jeongmin Lee. Study concepts: Jeongmin Lee, Sung Hun Kim. Study design: Jeongmin Lee, Sung Hun Kim. Definition of intellectual content: Jeongmin Lee, Sung Hun Kim. Literature research: Jeongmin Lee. Clinical studies: Jeongmin Lee, Sung Hun Kim, Bong Joo Kang. Experimental studies: NA. Data acquisition: Jeongmin Lee, Sung Hun Kim, Bong Joo Kang. Data analysis: Jeongmin Lee, Sung Hun Kim. Statistical analysis: Jeongmin Lee, Bong Joo Kang. Manuscript preparation: Jeongmin Lee, Sung Hun Kim, Bong Joo Kang. Manuscript editing: Jeongmin Lee, Sung Hun Kim, Bong Joo Kang. Manuscript review: Jeongmin Lee, Sung Hun Kim, Bong Joo Kang.

Competing interests

The authors declare no competing interests.

Additional information

Correspondence and requests for materials should be addressed to S.H.K.

Reprints and permissions information is available at www.nature.com/reprints.

Publisher's note Springer Nature remains neutral with regard to jurisdictional claims in published maps and institutional affiliations.



Open Access This article is licensed under a Creative Commons Attribution 4.0 International License, which permits use, sharing, adaptation, distribution and reproduction in any medium or format, as long as you give appropriate credit to the original author(s) and the source, provide a link to the Creative Commons license, and indicate if changes were made. The images or other third party material in this article are included in the article's Creative Commons license, unless indicated otherwise in a credit line to the material. If material is not included in the article's Creative Commons license and your intended use is not permitted by statutory regulation or exceeds the permitted use, you will need to obtain permission directly from the copyright holder. To view a copy of this license, visit <http://creativecommons.org/licenses/by/4.0/>.

© The Author(s) 2020